IEEE Access
Multidisciplinary | Rapid Review | Open Access Journal

Received May 9, 2019, accepted June 12, 2019, date of publication June 19, 2019, date of current version July 22, 2019.

Digital Object Identifier 10.1109/ACCESS.2019.2923746

Neural Network-Based Diagnostic Tool for Detecting Stator Inter-Turn Faults in Line Start Permanent Magnet Synchronous Motors

LUQMAN S. MARAABA[1], ZAKARIYA M. AL-HAMOUZ[2], (Senior Member, IEEE), ABDULAZIZ S. MILHEM[3], AND M. A. ABIDO[3,4], (Senior Member, IEEE)

[1]Center for Engineering Research, Research Institute, King Fahd University of Petroleum and Minerals, Dhahran 31261, Saudi Arabia
[2]School of Technology, Electrical Engineering Program, Michigan Technological University, Houghton, MI 1400, USA
[3]Department of Electrical Engineering, King Fahd University of Petroleum and Minerals, Dhahran 31261, Saudi Arabia
[4]K. A. Care Energy Research & Innovation Center, Dhahran 11451, Saudi Arabia

Corresponding author: Luqman S. Maraaba (lmaraaba@kfupm.edu.sa)

This work was supported by the King Abdul-Aziz City for Science and Technology (KACST), which was received via the Science and Technology Unit at King Fahd University of Petroleum and Minerals (KFUPM) through Project 13-ENE403-04.

ABSTRACT Three-phase line-start permanent magnet synchronous motors are considered among the most promising types of motors in industrial applications. However, these motors experience several faults, which may cause significant financial losses. This paper proposed a feed-forward neural network-based diagnostic tool for accurate and fast detection of the location and severity of stator inter-turn faults. The input to the neural network is a group of representative statistical and frequency-based features extracted from the steady-state three-phase stator current signals. The current signals with different numbers of shorted turns and loading conditions are captured using the developed finite element JMAG^{TM} model for interior mount LSPMSM. In addition, an experimental set-up was built to validate the finite element model and the proposed diagnostics tool. The simulation and experimental test results showed an overall accuracy of 93.125% in detecting the location and the size of inter-turn, whereas, the accuracy in detecting the location of the fault is 100%.

INDEX TERMS Electric motors, fault currents, fault detection, finite element analysis.

I. INTRODUCTION

In recent decades, faults in electric motors have been considered a major issue in industry. Production processes presume reliable and continuous operation of electric motors. However, motors are subject to many possible fault types. These faults may become catastrophic if not detected early. They may lead to complete motor failure [1]–[3], which interrupts the production process. These interruptions are costly in terms of maintenance and loss of production time. Therefore, having a fault-monitoring system is very important and increases the reliability and availability of electric machines. Detecting irregularity in a motor early using a proper fault diagnosis scheme will help prevent expensive failures (and, hence, prevent machine damage and reduce maintenance costs) and, more importantly, prevent unscheduled downtime that results in the loss of production time and income [4]–[6].

To save electricity, researchers focus on investigating and improving the efficiency of electric motors in manufacturing processes. Induction motors are among the motors most commonly used in industry; however, they suffer from low operational efficiency and low power factor. In contrast, permanent magnet synchronous motors are more efficient and powerful; however, they lack the starting capability of induction motors. Alternatively, line-start permanent magnet synchronous motors (LSPMSMs) have the following significant advantages over the two previously mentioned motors: high operational efficiency, high power factor, and the ability to self-start [7]–[9].

The LSPMSM is a hybrid electric motor and it has different aspects compared with PMSM. In LSPMSM starting, the induction torque, generated due to the induced current in

The associate editor coordinating the review of this manuscript and approving it for publication was Jiansong Liu.

the rotor bars, forces the rotor to rotate whereas the excitation torque generated by the permanent magnets acts as a braking torque. In PMSM, the motor needs an additional mean to start. On the other hand, In LSPMSM, at steady state, the motor rotates due to excitation and reluctance torque whereas the induction torque is zero with constant load. However, at steady state and under load variation, the bars of the squirrel cage work as dampers. While, in PMSM there is no induction torque even with variable loads, the main torque is the excitation torque. On the other hand, the LSPMSM suffers from demagnetization of permanent magnets due to the high starting current. Such differences in performance makes the fault detection in LSPMSM is more challenging task compared to induction motor and PMSM.

LSPMSMs experience several types of fault due to unavoidable mechanical and electrical stresses during operation, with the following representing the major faults: broken bars, eccentricity, bearing faults, stator inter-turn faults, demagnetization and broken end rings [10]–[13]. In the literature [14], [15], stator winding faults in machines have been reported to account for approximately 36% of motor faults. The main causes of stator winding faults are inefficient cooling systems, voltage stress, overloading, short circuits in the winding, chemical contamination and partial discharge in the winding. In most cases, stator winding faults start as turn-to-turn (inter-turn), coil-to-coil, phase-to-ground, or phase-to-phase faults, which ultimately lead to motor failure. It is crucial to develop an effective tool for detecting such faults in the initial stage because they become increasingly severe over time if they are not addressed [16]–[20].

Accurate modeling of electric motors is considered the first step in the detection and recognition of motor abnormalities [9]. Modeling electric motors during faults will also help in investigating the behavior and performance of motors. Based on the literature, two approaches are used for modeling motors during faults: analytic (electrical or magnetic)-based and finite element-based approaches [15], [21]. Because the use of LSPMSMs in industry is in its infancy, few papers on modeling LSPMSMs during faults are available. In [12], the performance of an LSPMSM with static eccentricity, dynamic eccentricity and mixed eccentricity was investigated using finite element models (FEMs). ANSYS Maxwell® was used to develop transient models of the motor. The speed, torque and flux density were recorded. The authors in [12] found that the static eccentricity has no effect on the motor performance under full load while the dynamic eccentricity has the main dominate effect. But the authors didn't investigate the effect of eccentricity (static and dynamic) under the variable loads which could affect their result. In [9], a mathematical model of an LSPMSM with asymmetrical stator winding was developed. The model was developed based on the principles of coupled magnetic circuit theory, electromechanical energy conversion and reference frame theory. Using the derived model, the case of stator winding asymmetry can be detected. But the torque equation and the permanent flux equations needs some modifications to include the effect of variable number of turns. In [22], a mathematical model of a LSPMSM experiencing demagnetization was developed using dq-axis, and the developed model was used to investigate the machine performance with demagnetization. The reversable or irreversible demagnetization (partial or complete) is highly related to temperature. However, this effect can't be investigated using the developed model. In [13], ANSYS Maxwell®was used to develop a model of a LSPMSM under broken bars fault. The authors in [13] found that the statistical features extracted from the envelope of stator current help in detecting broken bars fault. However, these features could be affected by other types of faults which make the use of them for discriminating between broken bar and other faults difficult.

Several signals can be used to indicate fault occurrence. Among these indicators are the magnetic flux, the vibration, the stator current (a negative and zero sequence or a third harmonic component), the zero-sequence component of the voltage, the thermal image, the instantaneous real and reactive power, the phase shift between the stator current and the supply voltage and the acoustic noise [23]–[33]. The motor current shows promise for fault detection because it is already available from motor control services without the need for extra design or additional hardware. The current signal inherently contains valuable information regarding the machine's performance and operating conditions [1].

Preventive maintenance is always more desirable than corrective maintenance. A substantial number of research efforts worldwide have been devoted to developing incipient fault diagnostic techniques. A neural network is a tool that plays an important role in developing online and offline diagnostic tools for motors, generators, transmission lines, cables and transformers [34]–[37]. In [38], a feed-forward neural network-based tool for detecting inter-turn faults in permanent magnet synchronous motors was proposed. The inputs to the proposed neural network were the first, third and fifth frequency components of the motor's current, and the neural network had 13 binary outputs, each of which represented an inter-turn fault severity level. Training and testing data were collected under different loading conditions and combinations of speed and inter-turn severity. The results demonstrated the success of the artificial neural network (ANN) at fault diagnosis. It is worth mentioning that the authors in [38] have tested the developed neural network with fault severities up to 25%. Where 25% severity is considered high and could affected the performance of the permanent magnets of the motor and the tool performance. In [39], a neural network-based diagnostic tool for detecting the location of an inter-turn fault in an induction motor was developed. The discrete wavelet transform was used for extracting representative features of the fault. The developed tool effectively detected the fault and it is location under different loading conditions, while the severity of the fault can't be detected using it. In [40], a tool for detecting the severity of inter-turn faults in permanent magnet synchronous motors was developed. The developed tool was neural network-based and

used the magnitude of the third harmonic component of the current as an input. Its output was the inter-turn fault severity. The testing result shows high accuracy of the tool. However, the developed tool lacks the capability of detecting fault location. In [41], a neural network-based tool for detecting the inter-turn fault level in an induction motor was proposed. The tool used the sum of the absolute values of the differences in the peak values of phase currents from each half cycle as the input and the fault level as the output. In this tool of fault detection, since only one input is used, neural network became simpler and so training time is less. But it lacks the ability of detecting the location of fault.

The use of LSPMSMs in industry is in its infant. considering the up-to-date literature, no finite element-based models do exist for interior-mount LSPMSM under stator inter-turn fault. In addition, there exist no diagnostic tools that can predict the location and/or the number of shorted turns in the stator of LSPMSMs. To bridge this lack in research, a new general FEM based model was developed using JMAG and validated experimentally using a 1-hp interior-mount LSPMSM. The developed model was used to simulate the motor currents under different loading and inter-turn conditions that could occurs in single or multiple phases of the motor. Then the stator currents during steady state have been recorded and used for extracting a group of statistical and frequency-based fault features. These features are used in the design of the neural network based diagnostic tool. The developed neural network is capable of detecting the fault location and the number of shorted turns.

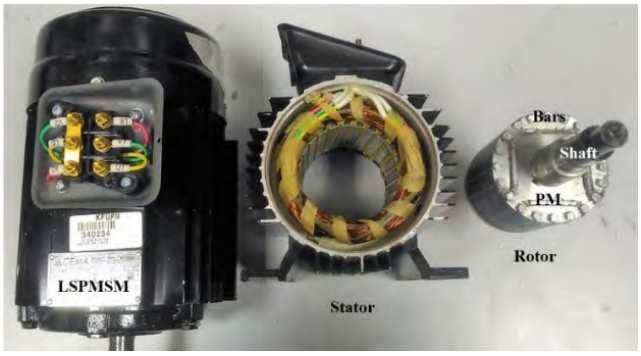

FIGURE 1. Interior-mount LSPMSM.

TABLE 1. LSPMSM parameters.

Parameter	Value
Mean air gap radius	37.35 mm
Number of poles	4
Air gap width	0.3 mm
Permanent magnet thickness	3 mm
Stack length	80 mm
Number of turns per stator phase	86 x 4
Rotor bar resistivity	2.655×10-8 Ω.m
Rotor end ring resistance	1×10-5 Ω
Angle between two adjacent rotor bars	18 degrees
Number of bars	20
Permanent magnet flux density	1.25 T
Machine rated power	1 hp
Moment of inertia	0.001586 kg.m2
Rated voltage	400 Vrms
Rated frequency	60 Hz
Rated speed	1800 rpm
Bar length	80 mm
Bar cross-sectional area	27 mm2

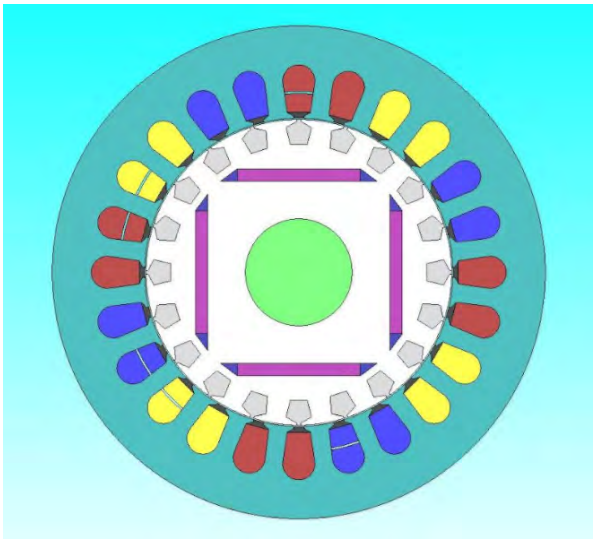

FIGURE 2. 2D geometry of the LSPMSM in JMAG^{TM}.

II. LSPMSM JMAG FAULT MODEL

Based on the literature and JMAG tutorials, as inter-turn fault is symmetric on the axial axis of the motor, it will be sufficient to perform 2D FEM analysis. This is in conformity with many previous research works, which used 2D FEM to investigate motor performance under faults [42]–[44]. Therefore, in this paper, a 2D FEM of a 1 hp interior-mount LSPMSM with a stator inter-turn fault is created using JMAG. In this study, the fault is assumed to be phase-a, while the other phases remain healthy. Fig 1 shows the motor used in the study, and Table 1 summarizes the motor's parameters. To create the FEM, the motor geometry was drawn using AUTOCADTM and then imported into JMAGTM. Fig 2 shows the 2D model's geometry. Each of the stator's phases occupies 8 slots (phase-a occupies the red slots, phase-b occupies the yellow slots, and phase-c occupies the blue slots). The Fig clearly shows that one pair of each of the phases slots is split into two parts: the inner part contains the healthy turns of the faulty phase coil, and the outer part contains the faulty turns of the same coil. After the geometry has been created, the material for each part of the motor is selected. Table 2 shows the materials of the motor parts.

To implement the electrical functionality in the 2D geometric model, the rotor and stator are linked to a circuit model.

TABLE 2. LSPMSM parts materials.

Component	Material
Stator core	Stainless steel
Stator lamination	50JN600 - Silicon steel
Stator coils	Copper
Rotor magnets	Recoma-24HE
Rotor bars	Aluminum Al99.7
Rotor lamination	50JN600 - Silicon steel
Shaft	Steel
Air gap	Air

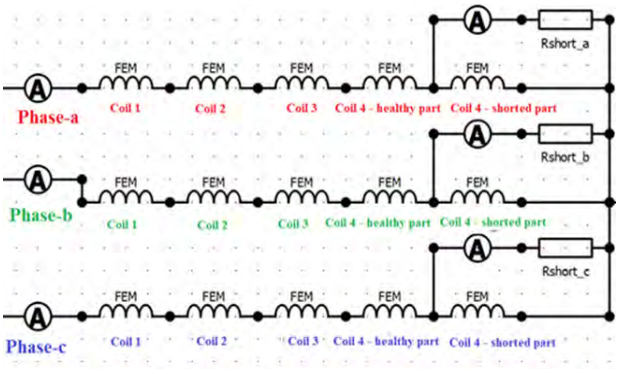

FIGURE 3. LSPMSM stator winding circuit.

The bars and end rings are linked to the rotor circuit, and the stator slots are linked to the stator circuit. Fig 3 shows the stator circuit. The Fig clearly shows that phase-a has four coils (coil 1 to coil 4). Coils 1, 2 and 3 are linked to the unsplit red slots of Fig 2; the healthy part of coil 4 is linked to the inner part of the split red slots; and the faulty part of coil 4 is linked to the outer part of the split red slots. The total number of turns in coil 4 (comprising both parts) is 86; therefore, it is easy to vary the number of shorted turns by changing the number of turns in the faulty part of coil 4. In order to limit the current in the shorted turns, an external resistance of 0.8 Ω is used. The same analogy goes for phase-b and –c.

In the finite element model developed in this work, several issues have been extended, developed, and generalized compared to the mathematical model developed in [15]. These are; using the developed finite element model the faults can be done in any of the phases or a combination of different phases as well as in a specific coil of the phases. In addition, unlike the mathematical model, the finite element model considers the location and distribution of windings in stator.

III. SIMULATION RESULTS AND EXPERIMENTAL VALIDATION

A. JMAG^{TM} MODEL TESTING AND EXPERIMENTAL VALIDATION

Using the developed JMAG^{TM}, the performance of the interior-mount LSPMSM with a stator inter-turn fault was investigated for different numbers of shorted turns and loads. To validate the results of the developed model, a 1-hp interior-mount LSPMSM motor was experimentally tested under healthy and faulty conditions. To introduce an inter-turn fault in the tested motor, three access points (A1, A2 and A3) were placed on coil 4 of phase-a, as shown in Fig 4. Using the access points, 26, 40 or 66 shorted turns were introduced in phase-a. in order to have fair comparison between the experimental and JMAG simulation results, an external resistance of 0.8-Ω is used to limit the fault current. Note that the external resistance in the simulation was 0.8 Ω, which was equal to the experimental external resistance (0.6 Ω)) plus 0.2 Ω (to represent the wire and the solder at the access point). A Cassy system (software, sensor, Profi-Cassy) and an isolation amplifier were used to measure the motor speed and the current response, as shown in the experimental setup of Fig 5.

FIGURE 4. The stator winding with access points.

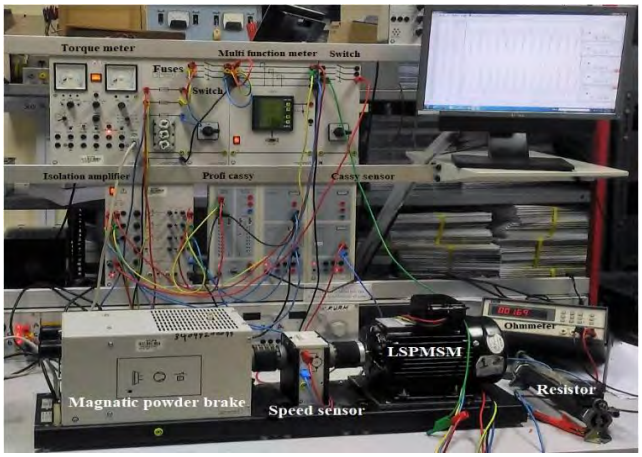

FIGURE 5. Experimental setup.

To verify the FEM, simulations and experimental tests were conducted with different numbers of shorted turns. The tested cases contained 0 (healthy), 26 and 40 shorted turns under no load. Both the current response and the speed were recorded, as shown in Figs 6 and 7, respectively. Fig 6 shows the phase-a current for three different cases. The Fig clearly shows that the results of the simulation and the experiment were almost the same in the steady state, with a small difference in the transient phase. Fig 7 shows the speed for the three cases. Clearly, the speed responses of the simulation and the experiment were in good agreement. Note that the ripples

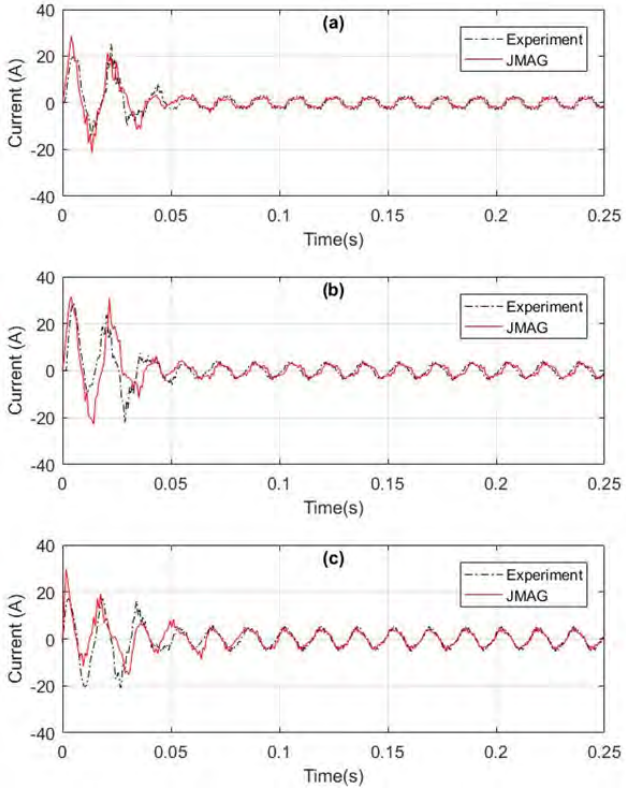

FIGURE 6. Phase-a stator current under no load (a) 0 shorted turns, (b) 26 shorted turns, and (c) 40 shorted turns.

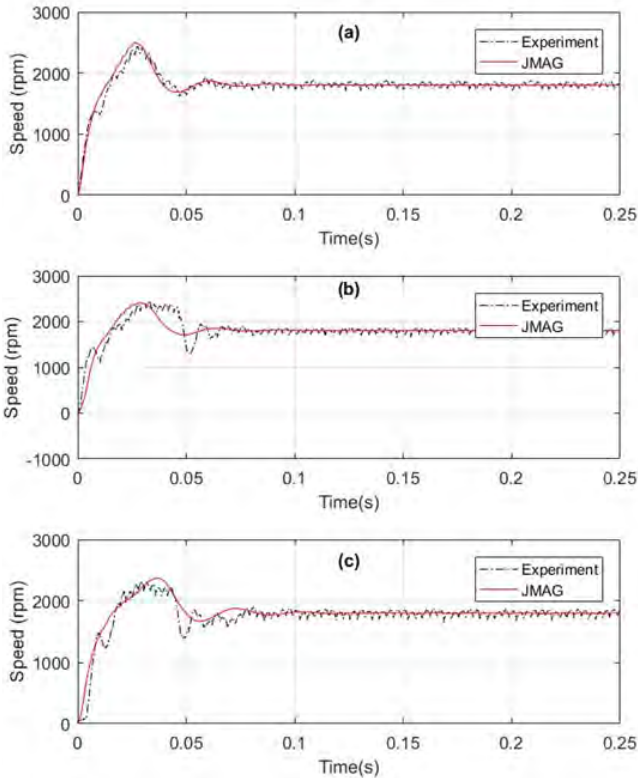

FIGURE 7. Rotor speed under no load (a) 0 shorted turns, (b) 26 shorted turns, and (c) 40 shorted turns.

in the steady-state speed response were caused by cogging torque and non-sinusoidal flux in the air gap (the turns were equally distributed across the slots) [45], [46]. However, the simulation and the experiment were in very good agreement. By looking at the current and speed signatures, it is clear that the current is more affected by inter-turn fault and hence the investigation will be focused on extraction features from current signals.

In this research work, no control strategies have been employed. The motor connected directly through data acquisition system to an AC power supply only as shown in figure 5. More details about the experimental setup are mentioned in reference [15]. It is worth mentioning that the motor run during steady state at synchronous speed (1800 rpm) even with 66 shorted turns (the largest fault size investigated in this paper). Moreover, 77 shorted turns case has been examined in the laboratory. It was observed that the motor is still able to run at synchronous speed under full loading condition.

B. EFFECT OF INTER-TURN FAULT ON STATOR CURRENTS

As the proposed diagnostic tool is expected to be used while the motor is running at steady state, the present section is aimed at investigating the effect of inter-turn fault on the motor steady state current. The FEM was used to simulate different shorted turns conditions. The results are shown in Figs 8-11. Fig 8 shows three phase stator currents and their frequencies spectrums under 28 shorted turns in phase-b

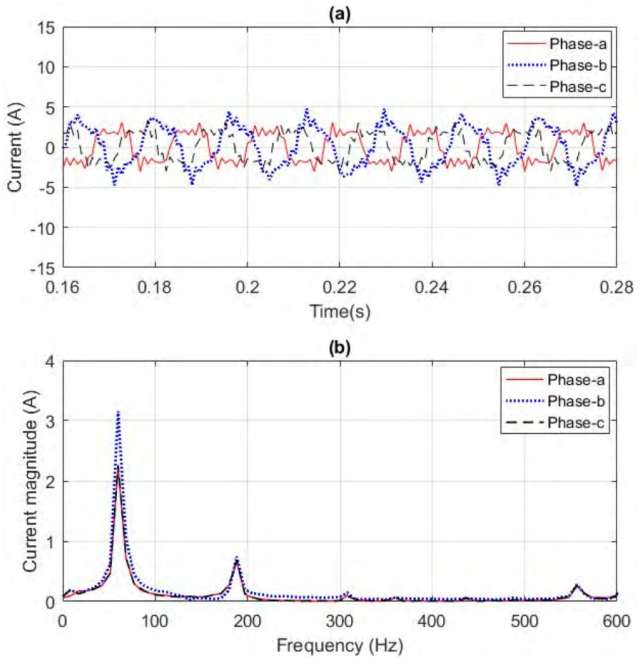

FIGURE 8. Three phase stator currents under 28 shorted turns in phase-b (a) time response and (b) frequency spectrum.

while the other two phases are healthy. The Fig shows a clear increase in phase-b current while the other two phases have a negligible change. For the case of 25 and 45 shorted turns in phases -a and –b, respectively, Fig 9 shows the three phase

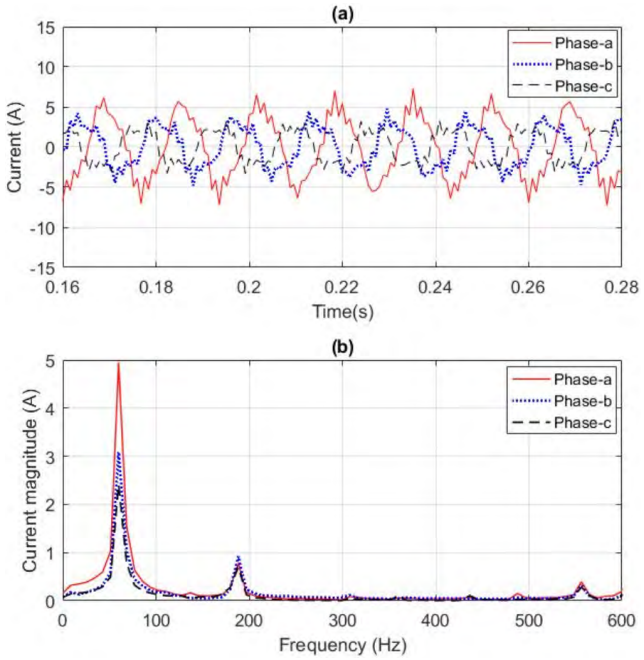

FIGURE 9. Three-phase stator currents under 25 and 45 shorted turns in phase-a and -b, respectively (a) time response and (b) frequency spectrum.

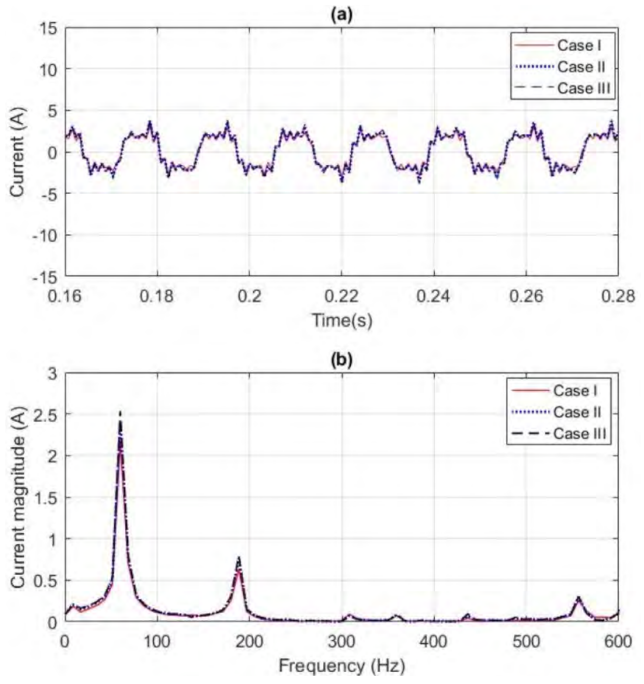

FIGURE 10. Phase-c current under no load (a) time response and (b) frequency spectrum.

stator currents and their frequencies spectrums. It is clear that the phases with shorted turns are clearly affected, and their magnitude of the fundamental current component is increased as the number of shorted turns increases. Fig 10 demonstrates clearly that the current time response and the corresponding frequency spectrum of the healthy phase is slightly affected by the occurrence of inter-turn fault in the other phases.

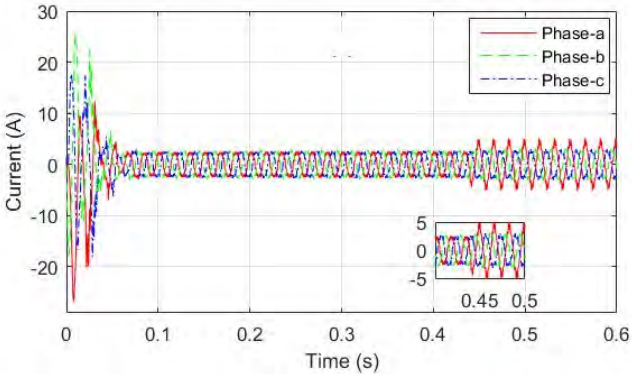

FIGURE 11. Experimental three phase stator current under no load.

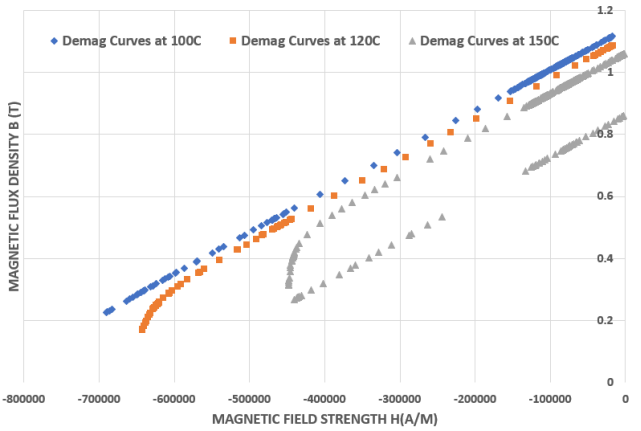

FIGURE 12. Demagnetization curves under 66 shorted turns.

The Fig shows three cases (case1- healthy condition, case 2- 42 shorted turns in phase-b, case 3- 25 and 45 shorted turns in phase-a and -b, respectively).

In order to confirm that the occurrence of inter-turn fault highly affects the phase it takes place in and slightly affects the other two phases, Fig 11 shows the experimental three phase current under no load for 26 shorted turns in phase-a occurring at 0.45 sec. It is clear from the Fig that, during fault, phase-a current is largely affected while other phases are slightly changed which confirms the simulation results. It is worth mentioning that having high number of shorted turns can cause demagnetization of the permanent magnets. However, the magnets of the used motor are Sintered Neodymium Iron Boron (NdFeB) Magnet batch N38SH. These magnets have very low knee point on their demagnetization curve. Demagnetization study has been carried on the motor magnets in presence of 66 shorted turns fault with full load applied on the motor. The demagnetization study done at the edge of the magnet at three temperature levels (100°C, 120°C and 150°C). The demagnetization curves are shown in figure 12. There was no any sign of demagnetization at 100°C. The operating point at 120°C was lower but didn't cross the knee point and accordingly no demagnetization occurred. However, the demagnetization curve at 120° C, shows the tendency to formulate demagnetization

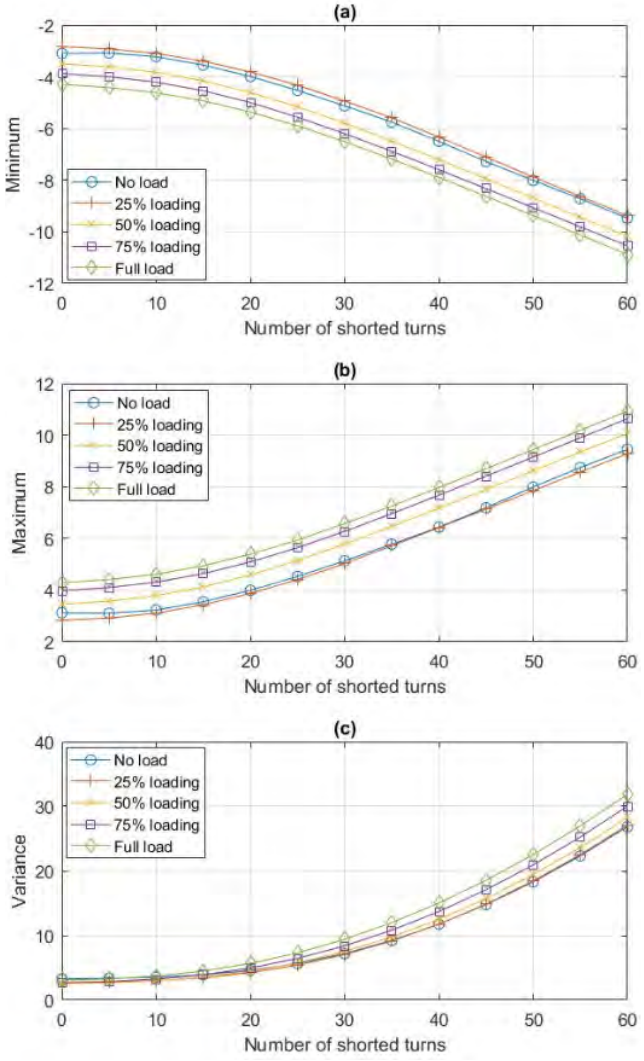

FIGURE 13. Extracted features: (a) minimum, (b) maximum, (c) variance.

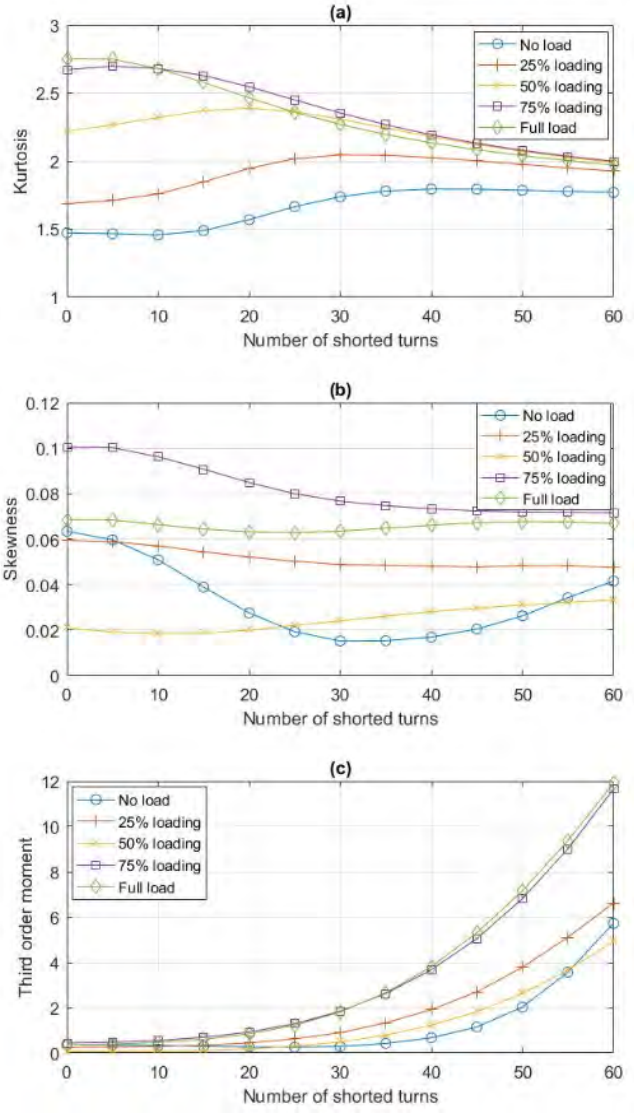

FIGURE 14. Extracted features (a) kurtosis (b) skewness, (c) third order momentum.

in the magnets. The curve at 150° C shows demagnetization case. Hence, we can conclude that demagnetization could take place at temperatures higher than 120° C in presence of 66 shorted turns.

IV. FEATURES EXTRACTION

In this section, several statistical and frequency-based features were extracted from the steady state current response. The extracted features were investigated to select the most representative features of the fault. The time-based features extracted were the maximum, minimum, variance, kurtosis, skewness, third-order moment, root mean square (RMS) and entropy. The frequency-based features were the amplitudes of the fundamental, second and third current components. For feature extraction, the developed FEM was simulated for different number of shorted turns and loading. For demonstration purposes, both statistical and frequency-based features shown in Figs 13-17 are extracted from phase-a for 65 simulated cases.

To investigate the frequency-based features, the frequency response of the current at full load for 0 (healthy), 26 and 40 shorted turns is shown in Fig 16. The Fig clearly shows that the fundamental component of the current is strongly affected by the fault size, whereas the other components are slightly affected. Therefore, the amplitude of the fundamental component of the current is selected as a representative fault feature. Fig 17 shows the fundamental component for the 65 simulated cases.

V. NEURAL NETWORK BASED DIAGNOSTIC TOOL

ANN has been implemented for diagnosis and classifications in several disciplines with impressive success. In this work, ANN has been trained offline to learn different types of motor faults. Ultimately, the trained ANN can be implemented to predict accurately the type and severity of the fault based on online measurements. This type of detection is considered

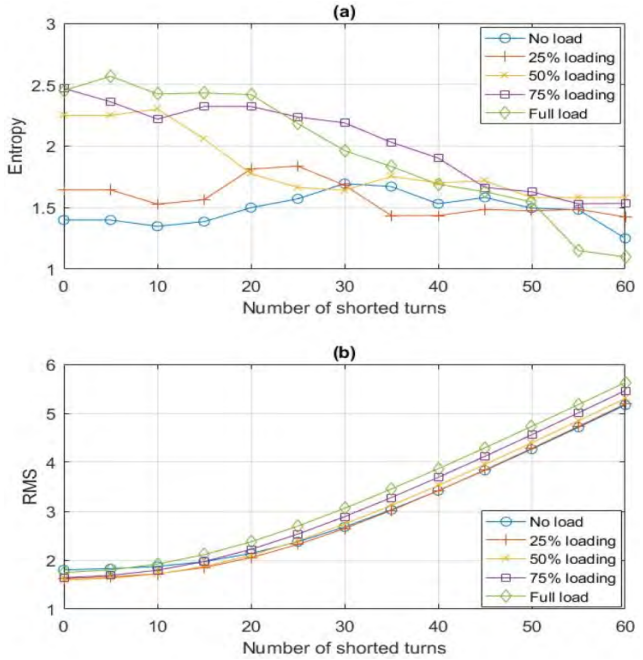

FIGURE 15. Extracted features (a) entropy and (b) RMS.

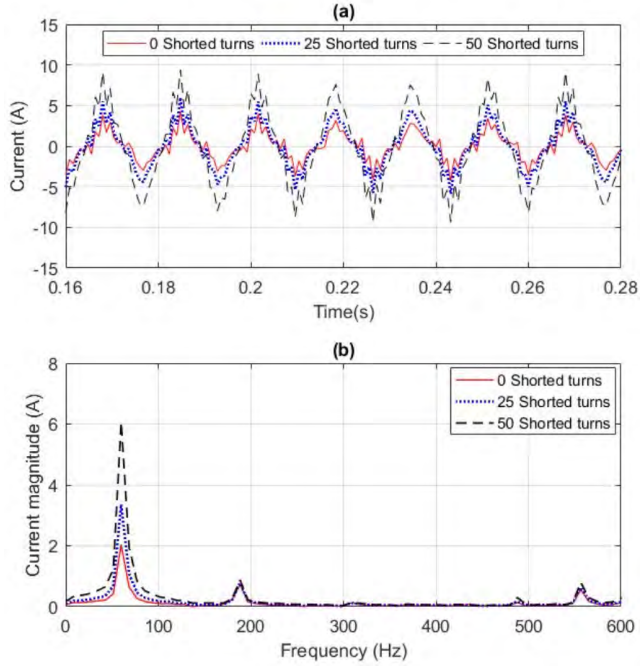

FIGURE 16. Phase-a current under full load: (a) time response and (b) frequency spectrum.

inexpensive and noninvasive. The most commonly used neural network for classification purposes is the multi-layer feed-forward neural network (MFNN). The feed-forward NN has the ability to learn various types of complex linear and nonlinear functions.

In developing the neural network, well-known statistical features such as: variance, skewness, kurtosis, third order momentum, entropy, maximum, minimum and (RMS) and

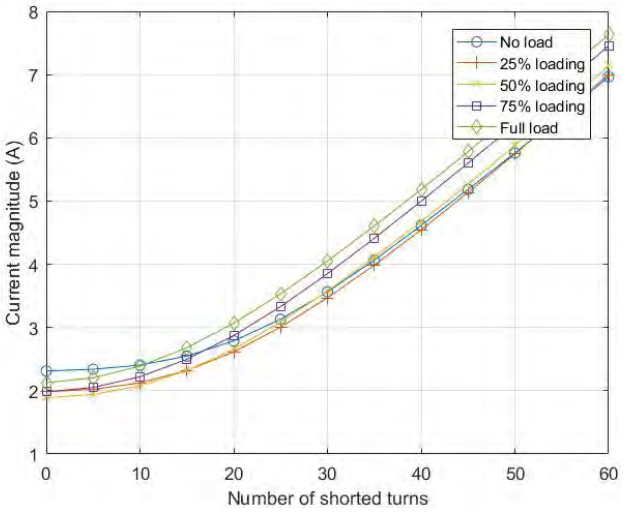

FIGURE 17. Magnitude of the fundamental component of the phase-a current.

fundamental current component for each phase have been examined. The testing performance has been monitored for different combination of these features. The skewness and entropy were found to have less significant contribution to the neural network performance. Therefore, as a compromise between the neural network performance and complexity, the other seven features are used. Moreover, Figs 13-17 show that the nonlinearity of the skewness and entropy are very high compared with those of other features. In addition, all the statistical features except skewness and entropy almost follow a certain pattern regardless of the load. Moreover, Fig 14-b clearly shows that little change in the skewness is observed as the number of shorted turns increases.

In addition, different structures of neural networks with different number of hidden layers and hidden neurons have been used to form suboptimal feed forward neural networks that correlate the extracted features with its corresponding number of shorted turns. The simplest with the highest efficiency was the one with two hidden layers with 18 and 5 neurons, respectively. It is worth mentioning that the stator current signals during steady state has been used as a fault indicator. Where the distinct fault features are extracted from the current signal. In this work, 3 cycle of the current signal (50ms in 60-Hz system) is found enough for extracting the correct representative features.

The outputs to the developed neural network are 3 which represent the number of shorted turns in each phase, and the inputs are 21 (the maximum, minimum, variance, kurtosis, third-order moment, (RMS) and fundamental current component for each phase). Fig 18 shows the topology of the designed neural network.

The activation function of all the neurons is 'tansig.'. 391 simulated cases are used to train the ANN. These represent inter-turn faults on any single phase or inter-turn faults in two phases at the same time. 160 unseen cases (captured experimentally and by JMAG simulation) are used to test

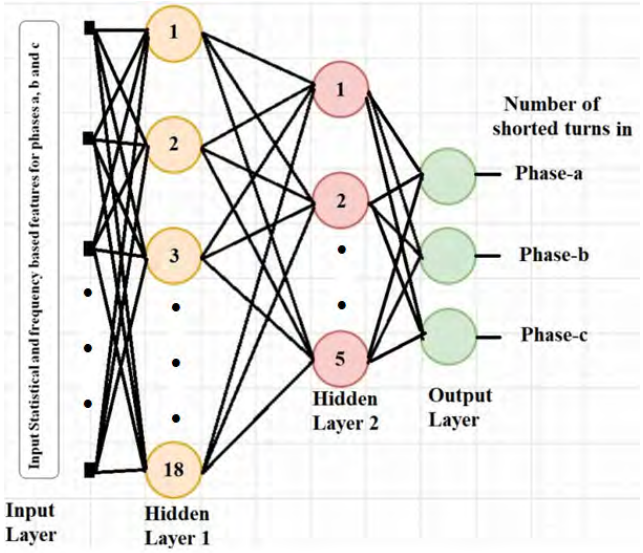

FIGURE 18. Neural network topology.

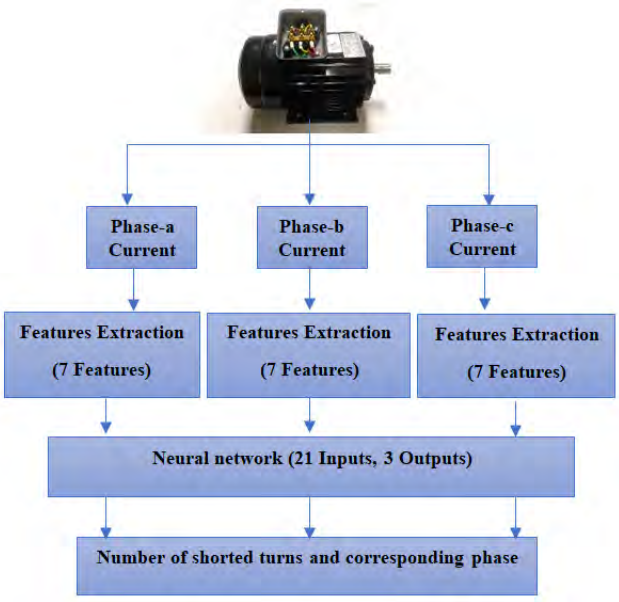

FIGURE 19. Diagnostic tool block diagram.

the ANN. For training, 13 numbers of shorted turns (0, 5, 10, 15, 20, 25, 30, 35, 40, 45, 50, 55, and 60) and 9 loading conditions (no load, 0.5N.m, 1N.m, 1.5N.m, 2N.m, 2.5N.m, 3N.m, 3.5N.m and 4N.m) are used. On the other hand, the number of shorted turns and loading values are taken different than the ones used in the training process. The neural network was trained using Levenberg–Marquardt backpropagation algorithm.

The proposed fault detection and classification technique starts with data acquisition and then application of fast Fourier transform and signal processing methods. There features are fed to the trained neural network in order to predict the location and number of shorted turns. This is illustrated in Figure 19. Table 3 shows a sample of the 160 testing cases used.

TABLE 3. Test results.

#	Load N.m	Actual shorted turns			Detected shorted turns			T/F detection			
		A	B	C	A	B	C	A	B	C	Detection
1	-0.25	4	0	0	1	0	0	F	T	T	F
2	-0.75	8	0	0	9	0	0	T	T	T	T
3	-1.25	13	0	0	14	0	0	T	T	T	T
4	-1.75	17	0	0	17	0	0	T	T	T	T
5	-2.25	22	0	0	22	0	0	T	T	T	T
6	-2.75	27	0	0	27	0	0	T	T	T	T
7	-3.25	33	0	0	33	0	0	T	T	T	T
8	-3.75	37	0	0	38	0	0	T	T	T	T
9	-0.25	41	0	0	41	0	0	T	T	T	T
10	-0.75	44	0	0	44	0	0	T	T	T	T
12	-0.75	0	8	0	0	8	0	T	T	T	T
13	-1.25	0	13	0	0	13	0	T	T	T	T
14	-1.75	0	17	0	0	17	0	T	T	T	T
15	-2.25	0	22	0	0	22	0	T	T	T	T
16	-2.75	0	27	0	0	27	0	T	T	T	T
17	-3.25	0	33	0	0	33	0	T	T	T	T
18	-3.75	0	37	0	0	37	0	T	T	T	T
19	-0.25	0	41	0	0	41	0	T	T	T	T
20	-0.75	0	44	0	0	44	0	T	T	T	T
21	-1.75	0	0	18	0	0	18	T	T	T	T
22	-2.25	0	0	14	0	0	13	T	T	T	T
23	-2.75	0	0	9	0	0	10	T	T	T	T
24	-3.25	0	0	3	0	0	0	T	T	F	F
25	-3.75	0	0	52	0	0	52	T	T	T	T
26	-2.75	0	0	33	0	0	33	T	T	T	T
27	-3.25	0	0	44	0	0	44	T	T	T	T
28	-0.0	8	15	0	10	15	0	T	T	T	T
29	-0.75	54	15	0	53	12	0	T	F	T	F
30	-1.75	8	22	0	10	22	0	T	T	T	T
31	-0.0	54	0	22	53	0	22	T	T	T	T
32	-2.75	8	0	35	11	0	35	F	T	T	F
33	-3.25	54	0	36	54	0	38	T	T	T	T
34	-0.0	39	0	43	40	0	42	T	T	T	T

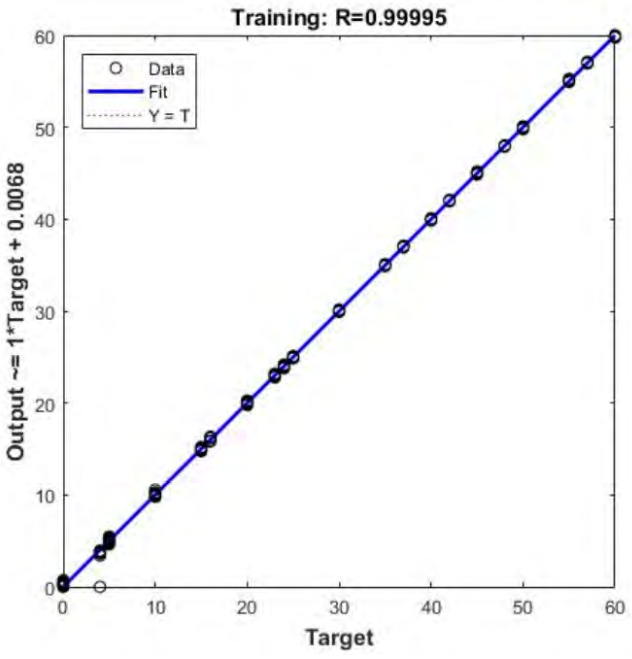

FIGURE 20. Neural network training regression.

The criterion of assuming a true (T) detection of the location and the number of shorted turns is as follows: the detection is true if the faulty phase(s) is correctly located and

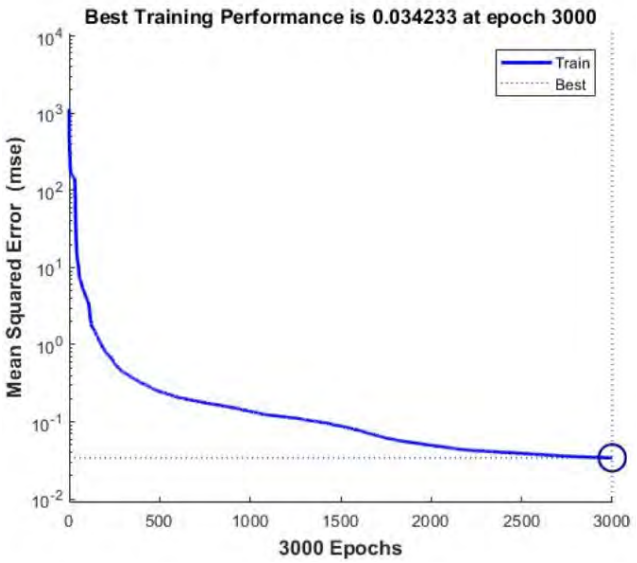

FIGURE 21. Neural network training performance.

TABLE 4. Electric motors diagnostic tools.

Reference	Motor Type	Current analysis	Minimum fault severity %
[47]	PMSM	Current harmonic components	4.17%
[48]	Induction	Stator current-Multiple reference frames theory	2.04%
[49]	Induction	Stator current-Wavelet transform Analysis	1.5%
[50]	PMSM	Stator current-Wavelet transform Analysis	2.78%
[51]	PMSM	Empirical mode decomposition (EMD) and Quadratic time–frequency (TF) analysis of stator current	2.78%

the difference between the predicted and actual number of shorted turns is less or equal to 2 turns. Otherwise if any of these two conditions is not satisfied then the detection is false (F).

The training accuracies are 97.186% and 100% for detecting the number of shorted turns and location, respectively. In testing phase, the accuracies with unseen cases are 93.125% and 100% for detecting the number of shorted turns and location, respectively. Figs. 20 and 21 shows the training phase regression and performance, respectively.

The minimum fault severity where the proposed tool detect correctly is 2.3% (8 turns) when fault occurs in one phase and 4.3% (15 turns) when fault occurs in two phases. Results are quite satisfactory compared to the other developed tools reported in the literature for other motors, as shown in Table 4. However, this comparison is somehow unfair since the construction and behavior of LSPMSM is different from PMSM and induction motors.

VI. CONCLUSION

In this paper, an FEM based model of an interior-mount LSPMSM with stator inter-turn fault was developed. In addition, an experimental test rig was implemented to validate the FEM model. The simulated and experimental steady state stator currents showed that the occurrence of inter-turn fault highly affects the phase it takes place in and slightly affects the other phases. This confirms the advantage of using the current signature as a fault indicator. Several statistical and frequency based features (maximum, minimum, variance, kurtosis, skewness, third-order moment, RMS, entropy and fundamental current component) were extracted from the current for different load levels and different inter-turn faults. All features except skewness and entropy follow a certain pattern regardless of the load and number of shorted turns. These distinct features were used in developing a feed forward neural network diagnostics tool capable of accurately predicting the location and number of shorted turns. The accuracy of the developed tool was confirmed by testing 160 unseen cases (shorted turns in one phase or two phases with different loading levels). The overall accuracy in detecting the number of shorted turns and its phase location is 93.125% whereas the accuracy in detecting the location of fault is 100%.

REFERENCES

[1] S. Choi, M. S. Haque, A. Arafat, and H. A. Toliyat, "Detection and estimation of extremely small fault signature by utilizing multiple current sensor signals in electric machines," *IEEE Trans. Ind. Appl.*, vol. 53, no. 3, pp. 2805–2816, May/Jun. 2017.

[2] S. Choi, E. Pazouki, J. Baek, and H. R. Bahrami, "Iterative condition monitoring and fault diagnosis scheme of electric motor for harsh industrial application," *IEEE Trans. Ind. Electron.*, vol. 62, no. 3, pp. 1760–1769, Mar. 2015.

[3] A. Gandhi, T. Corrigan, and L. Parsa, "Recent advances in modeling and online detection of stator interturn faults in electrical motors," *IEEE Trans. Ind. Electron.*, vol. 58, no. 5, pp. 1564–1575, May 2011.

[4] K. W. Lee, J. Hong, D. Hyun, S. B. Lee, E. J. Wiedenbrug, M. Teska, and C. Lim, "Detection of stator slot magnetic wedge failures for induction motors without disassembly," *IEEE Trans. Ind. Appl.*, vol. 50, no. 4, pp. 2410–2419, Jul./Aug. 2014.

[5] M. B. K. Bouzid, G. Champenois, N. M. Bellaaj, L. Signac, and K. Jelassi, "An effective neural approach for the automatic location of stator interturn faults in induction motor," *IEEE Trans. Ind. Electron.*, vol. 55, no. 12, pp. 4277–4289, Dec. 2008.

[6] D. C. Patel and M. C. Chandorkar, "Modeling and analysis of stator interturn fault location effects on induction machines," *IEEE Trans. Ind. Electron.*, vol. 61, no. 9, pp. 4552–4564, Sep. 2014.

[7] W. Fei, P. C. K. Luk, J. Ma, J. X. Shen, and G. Yang, "A high-performance line-start permanent magnet synchronous motor amended from a small industrial three-phase induction motor," *IEEE Trans. Magn.*, vol. 45, no. 10, pp. 4724–4727, Oct. 2009.

[8] J. Li, J. Song, and Y. Cho, "High performance line start permanent magnet synchronous motor for pumping system," in *Proc. IEEE Int. Symp. Ind. Electron.*, Jul. 2010, pp. 1308–1313.

[9] L. S. Maraaba, Z. M. Al-Hamouz, and M. A. Abido, "Modeling and simulation of line start permanent magnet synchronous motors with asymmetrical stator windings," in *Proc. 42nd Annu. Conf. IEEE Ind. Electron. Soc.*, Oct. 2016, pp. 1698–1703.

[10] G.-H. Kang, J. Hur, H. Nam, J.-P. Hong, and G.-T. Kim, "Analysis of irreversible magnet demagnetization in line-start motors based on the finite-element method," *IEEE Trans. Magn.*, vol. 39, no. 3, pp. 1488–1491, May 2003.

[11] Z. Dogan, "The static eccentricity fault diagnosis in time domain at line start permanent magnet synchronous motor," *J. New Results Sci.*, vol. 5, pp. 88–95, 2016.

[12] M. M. Sedky, "Diagnosis of static, dynamic and mixed eccentricity in line start permanent magnet synchronous motor by using FEM," *Int. J. Elect., Robot., Electron. Commun. Eng.*, vol. 8, no. 1, pp. 29–34, Jan. 2014.

[13] M. R. Mehrjou, N. Mariun, M. Karami, N. Misron, and M. A. M. Radzi, "Broken rotor bar detection in LS-PMSMs based on statistical features analysis of start-up current envelope," in *Proc. IEEE 3rd Int. Conf. Smart Instrum., Meas. Appl. (ICSIMA)*, Nov. 2015, pp. 1–6.

[14] A. Singh, B. Grant, R. DeFour, C. Sharma, and S. Bahadoorsingh, "A review of induction motor fault modeling," *Electr. Power Syst. Res.*, vol. 133, pp. 191–197, Apr. 2016.

[15] L. S. Maraaba, Z. M. AlHamouz, and M. A. Abido, "Mathematical modeling, simulation and experimental testing of interior-mount LSPMSM under stator inter-turn fault," *IEEE Trans. Energy Convers.*, to be published. doi: 10.1109/TEC.2018.2886137.

[16] S. M. A. Cruz and A. J. M. Cardoso, "Rotor cage fault diagnosis in three-phase induction motors by extended Park's vector approach," *Electr. Mach. Power Syst.*, vol. 28, no. 4, pp. 289–299, 2000.

[17] W. Liu, L. Liu, I.-Y. Chung, D. A. Cartes, and W. Zhang, "Modeling and detecting the stator winding fault of permanent magnet synchronous motors," *Simul. Model. Pract. Theory*, vol. 27, pp. 1–16, Sep. 2012.

[18] J. A. Farooq, T. Raminosoa, A. Djerdir, and A. Miraoui, "Modelling and simulation of stator winding inter-turn faults in permanent magnet synchronous motors," *COMPEL-Int. J. Comput. Math. Elect. Electron. Eng.*, vol. 27, no. 4, pp. 887–896, Jul. 2008.

[19] T. Kawady, A. A. Afify, A. M. Osheiba, and A. I. Taalab, "Modeling and experimental investigation of stator winding faults in induction motors," *Electr. Power Compon. Syst.*, vol. 37, no. 6, pp. 599–611, May 2009.

[20] R. M. Tallam, T. G. Habetler, and R. G. Harley, "Transient model for induction machines with stator winding turn faults," in *Proc. IEEE Ind. Appl. Conf.*, Oct. 2000, pp. 304–309.

[21] C. Rojas, M. G. Melero, M. F. Cabanas, J. M. Cano, G. A. Orcajo, and F. Pedrayes, "Finite element model for the study of inter-turn short circuits in induction motors," in *Proc. IEEE Int. Symp. Diagnostics Electr. Mach., Power Electron. Drives*, Sep. 2007, pp. 415–419.

[22] X. Lu, K. L. V. Iyer, K. Mukherjee, and N. C. Kar, "Study and detection of demagnetization in line start permanent magnet synchronous machines using artificial neural network," in *Proc. 15th Int. Conf. Elect. Mach. Syst. (ICEMS)*, Oct. 2012, pp. 1–6.

[23] V. C. M. N. Leite, J. G. B. da Silva, G. F. C. Veloso, L. E. B. da Silva, G. Lambert-Torres, E. L. Bonaldi, and L. E. de Lacerda de Oliveira, "Detection of localized bearing faults in induction machines by spectral kurtosis and envelope analysis of stator current," *IEEE Trans. Ind. Electron.*, vol. 62, no. 3, pp. 1855–1865, Mar. 2015.

[24] K. N. Gyftakis, M. Drif, and A. J. M. Cardoso, "Thorough investigation of the third current harmonic in delta-connected induction motors suffering from a stator inter-turn fault," in *Proc. IEEE 10th Int. Symp. Diagnostics Elect. Mach., Power Electron. Drives (SDEMPED)*, Sep. 2015, pp. 7–13.

[25] M. Drif and A. J. M. Cardoso, "Stator fault diagnostics in squirrel cage three-phase induction motor drives using the instantaneous active and reactive power signature analyses," *IEEE Trans. Ind. Informat.*, vol. 10, no. 2, pp. 1348–1360, May 2014.

[26] M. Eftekhari, M. Moallem, S. Sadri, and M.-F. Hsieh, "A novel indicator of stator winding inter-turn fault in induction motor using infrared thermal imaging," *Infr. Phys. Technol.*, vol. 61, pp. 330–336, Nov. 2013.

[27] N. Lashkari, J. Poshtan, and H. F. Azgomi, "Simulative and experimental investigation on stator winding turn and unbalanced supply voltage fault diagnosis in induction motors using artificial neural networks," *ISA Trans.*, vol. 59, pp. 334–342, Nov. 2015.

[28] A. M. da Silva, R. J. Povinelli, and N. A. O. Demerdash, "Rotor bar fault monitoring method based on analysis of air-gap torques of induction motors," *IEEE Trans. Ind. Informat.*, vol. 9, no. 4, pp. 2274–2283, Nov. 2013.

[29] T. Kato, K. Inoue, and K. Yoshida, "Diagnosis of stator-winding-turn faults of induction motor by direct detection of negative sequence currents," *Electr. Eng. Jpn.*, vol. 186, no. 3, pp. 75–84, Feb. 2014.

[30] J. C. Urresty, J.-R. R. Ruiz, M. Delgado, and L. Romeral, "Detection of demagnetization faults in surface-mounted permanent magnet synchronous motors by means of the zero-sequence voltage component," *IEEE Trans. Energy Convers.*, vol. 27, no. 1, pp. 42–51, Mar. 2012.

[31] K. N. Gyftakis, D. V. Spyropoulos, J. C. Kappatou, and E. D. Mitronikas, "A novel approach for broken bar fault diagnosis in induction motors through torque monitoring," *IEEE Trans. Energy Convers.*, vol. 28, no. 2, pp. 267–277, Jun. 2013.

[32] P. C. M. L. Filho, R. Pederiva, and J. N. Brito, "Detection of stator winding faults in induction machines using flux and vibration analysis," *Mech. Syst. Signal Process.*, vol. 42, nos. 1–2, pp. 377–387, Jan. 2014.

[33] S. Jelassi, R. Romary, and J.-F. Brudny, "Vibro-acoustic behaviour of an induction machine with stator inter-turn short-circuit," *Eur. Phys. J. Appl. Phys.*, vol. 73, no. 1, Jan. 2016, Art. no. 10904.

[34] K. Zhang, F. Yuan, J. Guo, and G. Wang, "A novel neural network approach to transformer fault diagnosis based on momentum-embedded BP neural network optimized by genetic algorithm and fuzzy c-means," *Arabian J. Sci. Eng.*, vol. 41, no. 9, pp. 3451–3461, 2016.

[35] A. Prasad and J. B. Edward, "Importance of artificial neural networks for location of faults in transmission systems: A survey," in *Proc. 11th Int. Conf. Intell. Syst. Control (ISCO)*, Jan. 2017, pp. 357–362.

[36] A. Nag and A. Yadav, "Fault classification using artificial neural network in combined underground cable and overhead line," in *Proc. IEEE 1st Int. Conf. Power Electron., Intell. Control Energy Syst. (ICPEICES)*, Jul. 2016, pp. 1–4.

[37] W. Chine, A. Mellit, V. Lughi, A. Malek, G. Sulligoi, and A. M. Pavan, "A novel fault diagnosis technique for photovoltaic systems based on artificial neural networks," *Renew. Energy*, vol. 90, pp. 501–512, May 2016.

[38] S. S. Moosavi, A. Djerdir, Y. Ait-Amirat, and D. Khaburi, "ANN based fault diagnosis of permanent magnet synchronous motor under stator winding shorted turn," *Electr. Power Syst. Res.*, vol. 125, pp. 67–82, Aug. 2015.

[39] B. Bessam, A. Menacer, M. Boumehraz, and H. Cherif, "Wavelet transform and neural network techniques for inter-turn short circuit diagnosis and location in induction motor," *Int. J. Syst. Assurance Eng. Manage.*, vol. 8, pp. 478–488, Jan. 2017.

[40] F. Cira, M. Arkan, and B. Gumus, "Detection of stator winding inter-turn short circuit faults in permanent magnet synchronous motors and automatic classification of fault severity via a pattern recognition system," *J. Electr. Eng. Technol.*, vol. 11, no. 2, pp. 416–424, Mar. 2016.

[41] G. Rajamany and S. Srinivasan, "An artificial neural networks application for the automatic detection of severity of stator inter coil fault in three phase induction motor," *J. Electr. Eng. Technol.*, vol. 12, no. 6, pp. 2219–2226, Nov. 2017.

[42] B. Vaseghi, N. Takorabet, and F. Meibody-Tabar, "Fault analysis and parameter identification of permanent-magnet motors by the finite-element method," *IEEE Trans. Magn.*, vol. 45, no. 9, pp. 3290–3295, Sep. 2009.

[43] B. Vaseghi, N. Takorabet, B. Nahid-Mobarakeh, and F. Meibody-Tabar, "Modelling and study of PM machines with inter-turn fault dynamic model–FEM model," *Electr. Power Syst. Res.*, vol. 81, no. 8, pp. 1715–1722, Aug. 2011.

[44] J.-H. Choi, B.-G. Gu, and C.-Y. Won, "Modeling and analysis of PMSMs under inter turn short faults," *J. Electr. Eng. Technol.*, vol. 8, no. 5, pp. 1243–1250, Sep. 2013.

[45] E. Peralta-Sanchez and A. C. Smith, "Line-start permanent-magnet machines using a canned rotor," *IEEE Trans. Ind. Appl.*, vol. 45, no. 3, pp. 903–910, May 2009.

[46] Y. Bao, L. Liu, Y. Zhang, and X. Feng, "Performance investigation and comparison of line start-up permanent magnet synchronous motor with super premium efficiency," in *Proc. Int. Conf. Elect. Mach. Syst.*, Aug. 2011, pp. 1–6.

[47] K.-H. Kim, "Simple online fault detecting scheme for short-circuited turn in a PMSM through current harmonic monitoring," *IEEE Trans. Ind. Electron.*, vol. 58, no. 6, pp. 2565–2568, Jun. 2011.

[48] S. M. A. Cruz and A. J. M. Cardoso, "Multiple reference frames theory: A new method for the diagnosis of stator faults in three-phase induction motors," *IEEE Trans. Energy Convers.*, vol. 20, no. 3, pp. 611–619, Sep. 2005.

[49] P. S. Barendse, B. Herndler, M. A. Khan, and P. Pillay, "The application of wavelets for the detection of inter-turn faults in induction machines," in *Proc. IEEE Int. Electr. Mach. Drives Conf.*, May 2009, pp. 1401–1407.

[50] J. A. Rosero, L. Romeral, J. Cusido, A. Garcia, and J. A. Ortega, "On the short-circuiting fault detection in a PMSM by means of stator current transformations," in *Proc. IEEE Power Electron. Spec. Conf.*, Jun. 2007, pp. 1936–1941.

[51] J. A. Rosero, L. Romeral, J. A. Ortega, and E. Rosero, "Short-circuit detection by means of empirical mode decomposition and Wigner–Ville distribution for PMSM running under dynamic condition," *IEEE Trans. Ind. Electron.*, vol. 56, no. 11, pp. 4534–4547, Nov. 2009.

LUQMAN S. MARAABA was born in Qalqilia, Palestine, in 1987. He received the B.Sc. degree (Hons.) in electrical engineering from An-Najah National University, Nablus, Palestine, in 2010, and the M.Sc. and Ph.D. degrees in electrical engineering from the King Fahd University of Petroleum and Minerals (KFUPM), Dhahran, Saudi Arabia, in 2014 and 2018, respectively, where he is currently a Research Engineer III with the Center for Engineering Research Research Institute. His research interests include electric machine modelling, fault diagnostics, power systems, and high-voltage insulators.

ZAKARIYA M. AL-HAMOUZ received the B.Sc. degree in electrical engineering from Yarmouk University, Irbid, Jordan, in 1986, the M.Sc. degree in electrical engineering from the Jordan University of Science and Technology, in 1989, and the Ph.D. degree in electrical engineering from the King Fahd University of Petroleum and Minerals (KFUPM), Dhahran, Saudi Arabia, in 1994. He has a long experience in teaching undergraduate and graduate courses, supervising the M.Sc. and Ph.D. degree students, and senior level capstone design projects. From 1994 to 2017, he was a Faculty Member of the KFUPM. He is also a Faculty Member of the School of Technology, Electrical Engineering Program, Michigan Technological University, USA. His research efforts to date have led to the publication of 55 refereed journals and 53 conference papers. He holds five U.S. issued and two U.S. published patents. His current research interests include the diagnosis of failures in power components and power system control. He was a recipient of the IEEE/IAS James Melcher Prize Paper Award, in 1999, and the KFUPM Excellence in Research Award, in 2000.

ABDULAZIZ S. MILHEM was born in Jenin, Palestine, in 1983. He received the B.Sc. degree in electrical engineering from An-Najah National University, Nablus, Palestine, in 2006, and the M.Sc. degree in electrical engineering from the King Fahd University of Petroleum and Minerals (KFUPM), where he is currently pursuing the Ph.D. degree with the Electrical Engineering Department and currently involved in the construction of HV substations. His research interests include ac machines analysis and failures diagnosis using FEM software, renewable energy systems, power system analysis, and planning.

M. A. ABIDO (SM'15) received the B.Sc. (Hons.) and M.Sc. degrees in electrical engineering from Menoufia University, Shebin El-Kom, Egypt, in 1985 and 1989, respectively, and the Ph.D. degree from the King Fahd University of Petroleum and Minerals (KFUPM), Dhahran, Saudi Arabia, in 1997.

He is currently a Distinguished University Professor with KFUPM. He is also a Senior Researcher with the K.A.CARE Energy Research and Innovation Center, Dhahran. He has participated over 60 funded projects and supervised over 50 M.S. and Ph.D. students. He has published two books and more than 350 papers in reputable journals and international conferences. His research interests include power system control and operation and renewable energy resources integration to power systems. He was a recipient of the First Prize Paper Award of the Industrial Automation and Control Committee of the IEEE Industry Applications Society, in 2003, the Abdel-Hamid Shoman Prize for Young Arab Researchers in Engineering Sciences, in 2005, the Best Applied Research Award of the 15th GCC-CIGRE Conference, Abu-Dhabi, UAE, in 2006, the KFUPM Excellence in Research Awards, in 2002, 2007, and 2012, the KFUPM Best Project Award, in 2007 and 2010, and the Best Poster Award at the International Conference on Renewable Energies and Power Quality (ICREPQ'13), Bilbao, Spain, in 2013. He has received the Almarai Prize for Scientific Innovation 2017–2018, Distinguished Scientist, Saudi Arabia, in 2018, and the Khalifa Award for Education 2017–2018, Higher Education, Distinguished University Professor in Scientific Research, Abu Dhabi, in 2018.